Allende Xenolith AF: Undisturbed Record of Condensation and Aggregation of Matter in the Solar Nebula

G. Kurat*, H. Palme**, F. Brandstätter* and J. Huth**

* Naturhistorisches Museum, A-1014 Vienna, Austria
** Max-Planck-Institut für Chemie, D-6500 Mainz, FRG

Z. Naturforsch. **44a**, 988–1004 (1989); received August 14, 1989

Dedicated to Heinrich Wänke on the occasion of his 60th birthday

In this paper an unusual, cm-sized xenolith from the Allende meteorite is described. Xenolith Allende-AF (All-AF) is chemically similar to bulk Allende, its texture is, however, completely different. It consists mainly of highly porous silicate-rich aggregates embedded in a largely opaque matrix. Occasionally olivine-sulfide-metal aggregates and large sulfide-andradite objects are found. Chondrules are absent and grain size in matrix and aggregates is the same, quite different from normal Allende.

The main mineral in All-AF is olivine (22–41 wt% FeO), low Ca-pyroxene is absent, but a variety of clinopyroxenes were encountered. Rare phases found throughout All-AF are refractory metal nuggets (Ir, Os, Ru etc.), HgS, and Ca-phosphate. Associated with sulfide-andradite objects are native-Cu, Ti-magnetite, perovskite, barite, and calcite.

Morphology, crystalline state and minor element contents of olivine strongly suggest an origin by condensation from a gas. Al_2O_3-contents, for example, range from 0.5 to 3% and Cr_2O_3-contents reach 2.5%.

Texture of All-AF indicates that condensation of olivine continued during formation of aggregates. Relictic low-Fe aluminous diopsides suggest that olivine was initially FeO-poor. Before final accretion into a solid rock exchange reactions between condensed phases and an (increasingly oxidized) vapor established the high FeO-content of olivine. A similar process led to sulfurization of most of the original metal. The exotic sulfide-andradite objects are probably alteration products of unusual, metal-rich calcium-aluminium-rich inclusions.

It appears that All-AF has preserved a unique record of condensation, hierarchical aggregation, and metasomatic exchange reactions in the solar nebula.

1. Introduction

Lithic inclusions similar in composition to carbonaceous chondrites are common in C3 and C2 chondrites [1–6], in unequilibrated ordinary chondrites [7–11], and in ureilites [12]. They are very rare in equilibrated ordinary chondrites [13, 14], in mesosiderites [15], howardites [16, 17], and irons with silicate inclusions [18].

Most of such carbonaceous xenoliths are chemically similar – but not identical – to C3 chondrites [6, 19]. Their mineralogy, texture, and degree of oxidation, however, may be quite different from C3 chondrites. The most common carbonaceous xenoliths in carbonaceous chondrites have been named "dark inclusions" (DIs) [5]. This name covers a highly heterogeneous group of lithic inclusions. Textures range from chondritic, e.g. chondrules, aggregates, lithic and mineral fragments embedded in a fine-grained matrix, to fine-grained matrix-like aggregates without chondrules, lithic fragments, and CAIs. A classification scheme has been developed for DIs [20] which relates different textures and volatile element contents to different degrees of metamorphism and hydrothermal alteration. The direct connection to C3 chondrites is clearly supported by oxygen isotope data [21, 19, 22]. Individual DIs straddle the Allende mixing line up to fairly heavy oxygen isotope compositions approaching ureilite oxygen. The ureilite connection is further supported by the fact that the majority of DIs is dominated by olivine. They are also rich in carbon [23–25] and trapped noble gases, planetary noble gases and anomalous xenon (CCF-Xe) [23, 26].

In spite of the strong indication of a primitive origin of DIs by the noble gas data there exists a variety of genetic models based mainly on the regolith hypotheses of Fruland et al. [5], which was supported by Ott et al. [23], Bunch et al. [26], and Bunch and Chang [20]. It has been challenged by Heymann et al. [25] and Bischoff et al. [19] on chemical grounds, high C con-

Reprint requests to Dr. H. Palme, Max-Planck-Institut für Chemie, Saarstraße, D-6500 Mainz.

0932-0784 / 89 / 1000-0988 $ 01.30/0. – Please order a reprint rather than making your own copy.

tents and low alkali contents, respectively, both incompatible with a regolith origin.

We report here on a xenolith (All-AF) from the Allende carbonaceous chondrite which may be related to the common fine-grained DIs from Allende. However, it differs in several features from DIs described so far in the literature. The chemical composition of All-AF, for example, is in some respect complementary to that of DIs [22]. Also, All-AF does not fit the classification scheme of DIs [20]. We believe that All-AF is a new type of chondrite rock that has uniquely preserved records of processes which may have been responsible for the formation of chondrites and other meteorites. This is a first report on the petrology of this – as we believe – very important rock. Because the nature of this rock is so vastly different from all meteorites we know so far, the description has to be supported by an unusual amount of microphotographs and a detailed discussion of its constituents and their interrelationships. The implications of this study are far-reaching, and yet many detailed aspects of this rock and its constituents have to await further studies.

2. Description

During cutting of a 3 kg piece of Allende an angular fragment of unusual appearance was encountered [27, 28]. It has a rectangular cross section of about 1×2 cm and extended through several slices of 0.8 cm thicknesss each. The total volume of the inclusion amounted to about 3 cm^3. Macroscopically it appeared to be a fragment of a C3 chondrite which had experienced some alteration (Fig. 1) that led to the discoloration of all constituents: the fragment is dark brown in color. Based on this expertise the inclusion was called Allende "altered fragment" or *Allende-AF* (All-AF).

The rock macroscopically appears to consist of densly packed round, irregularly to lobate shaped silicate objects and a few sulfide-rich objects embedded in a dark matrix. Under the microscope All-AF appears to be principally an aggregate of aggregates (Figure 2). Fundamental differences between Allende and All-AF become apparent under the scanning electron microscope. Although the average size of aggregates in both rocks is about the same (Fig. 1), normal Allende consists of aggregates (and chondrules) containing coarse-grained olivine and pyroxene which are embedded in a fine-grained matrix. In All-AF, however, aggregates and matrix consist of olivines of roughly the same grain-size. These olivines are much coarser-grained than Allende matrix olivines.

The most common aggregates in All-AF are silicate-rich and consist mainly of olivine with minor amounts of nepheline and varying contents of sulfides and metal. Some exotic objects are present which comprise complex silicate-sulfide-metal aggregates, and sulfide-andradite-objects.

2.1. The Common Silicate-Rich Aggregates

2.1.1. The Constituents

The basic component of the ordinary aggregates and the matrix is *olivine*. This olivine is unusual in several respects. It has an exceptionally weak birefringence resulting in low order interference colors in thin sections of normal thickness. It has sectoral and undulous extinction with some individuals being highly disturbed. Sometimes it has a color even in thin section ranging from yellowish to yellow and yellowish-brown (macroscopically all olivines are brown). Grains are usually small but of platy shape with dimensions typically of some 5–10 to 30 μm. These olivines are considerably larger than those in the matrix of Allende (Figure 3). The olivine platelets, however, usually form a variety of larger units, mostly stacks of platelets in highly different sizes and different degrees of intergrowth of the individual platelets. Large stacks of such platelets are fairly common and display different degrees of intergrowth but always contain abundant pore space. These individual stacks cover a large range in sizes from 10 μm up to over 500 μm. The largest fluffy olivine stacks tend to develop rounded and densely intergrown surfaces (larger rounded objects in Fig. 2 and Figure 4). They form individual objects of chondrule-like appearance or they are parts of aggregates. Sometimes olivine stacks are partially intergrown in such a way as to form olivine bars (actually thick plates) perpendicular to the elongation of the original platelets. These bars reach thicknesses up to 30 μm and are themselves oriented parallel to each other strongly resembling "barred" olivines (BO) (Figure 5). The plates are oriented parallel to (010) as are the plates of common barred olivines in carbonaceous and ordinary chondrites.

Medium sized olivine stacks can either occur isolated or be part of medium to large sized aggregates. Small olivine stacks are present in aggregates and the

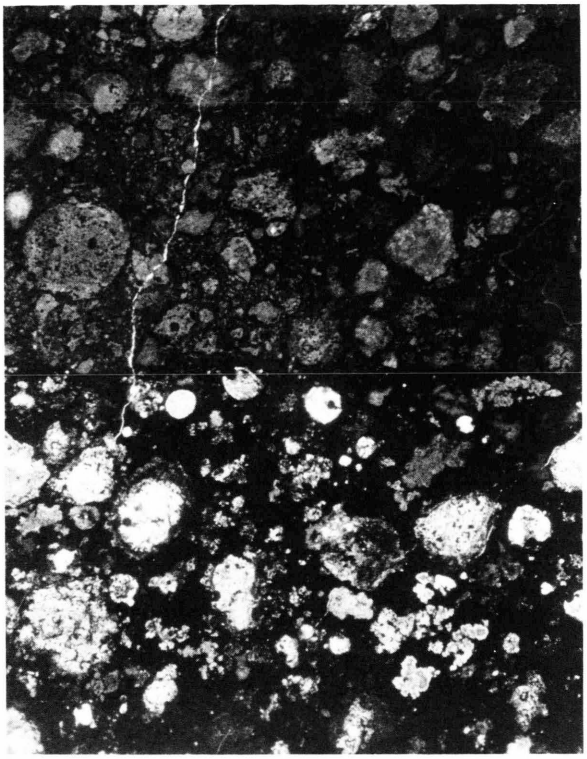

Fig. 1. Allende-AF (upper dark portion) and normal Allende (lower portion). The aggregate sizes are very much the same in both rocks. Normal Allende contains abundant coarse-grained, transparent minerals (mainly olivine) whereas all phases in All-AF are just translucent and brown in color. Transmitted light picture, length is 11.4 mm.

Fig. 2. Allendeg fragment All-AF, overview. Large aggregate of complex aggregates (e.g. in center) and mostly irregularly shaped aggregates in dark matrix. Transmitted light. Length of picture is 5 mm.

Fig. 3. Border between All-AF (lower portion) and normal Allende matrix (upper portion). Note the difference in grain-size, in the morphology of olivines and the Fe diffusion borders in the aggregate in normal Allende. Back scattered electron (BSE) picture, length is 310 μm.

Fig. 4. Portion of a large fluffy olivine stack. Subparallel plates of olivine are partially intergrown with each other, especially at the surface, where an almost continuous rim is formed. The pore space is partly filled by nepheline (medium grey). BSE picture. Length of picture is 260 μm.

matrix. With falling stack size the pore space is reduced up to the point where they look like small (< 10 μm) blocky olivine crystals (Figures 3, 4).

A different type of olivine occurs in large cavities and cracks in aggregates and the matrix: acicular crystals up to 30 μm long and 1–5 μm thick or bundles of such crystals fill this space (Figure 6). They tend to be oriented approximately perpendicular to the walls of the opening and fill it in as filthy, porous manner.

The second major component of the ordinary aggregates are *silicate-sulfide-metal objects*. They are themselves aggregates displaying a variety of morphological features. The simplest objects consist of an aggregate of olivine stacks which are covered and partially infiltrated by sulfide and metal (Figure 7). The most common type consists of densly intergrown granular to platy olivine, nepheline, sulfide, and metal covered by a discontinuous or continuous rim of sulfide and metal of variable thickness (Figures 3, 7). Porosities are generally low although there are some exceptions. However, in no case is the porosity as high as in the silicate-rich aggregates and the matrix.

The silicate-sulfide-metal aggregates are always rounded and range from almost spherical to complex lobate. They range from about 20 to 200 μm (Fig. 7) and predominantly occur in silicate-rich aggregates where they tend to be distributed in zones around a pure silicate core. Small objects of this type occur throughout silicate-rich aggregates and also in the matrix where sometimes small single stacks of olivine are covered by sulfide and metal.

The proportions of sulfides to metal are highly variable. Some objects contain solely metal whereas others contain only sulfides, even if they occur within the same silicat-rich aggregate. The majority contains both phases and if both are present they tend to be separated and located at opposite sides of the object. Pentlandite, $(Fe, Ni)_9S_8$, is the dominating sulfide phase, troilite, FeS, is less abundant. The metal phase is exclusively awaruite, Ni_3Fe.

Massive sulfide nodules are a rare constituent of silicate-rich aggregates. These mostly large (up to 800 μm) nodules consist of a core composed mainly of troilite, intergrown with fine-grained olivine and Ca-phosphate, surrounded by a discontinuous, dense rim (50–100 μm) of troilite and pentlandite (Figure 8). This rim includes abundant olivines near its surface and contact to the olivine aggregates. The core is irregular granular. Grain-sizes of the sulfides are highly variable ranging from a few μm up to over 50 μm. Sulfide grain-sizes in the rims are commonly large (50–100 μm) with the grain boundaries preferentially oriented perpendicular to the surface. Silicate and phosphate grain-sizes in both core and rim range from about 15 μm down to below 1 μm. In places, silicates and phosphates form fluffy, irregularly shaped aggregates that may contain abundant pore space.

Nepheline is an important constituent of all objects in All-AF. It never forms objects of its own but rather fills the pore space between olivine plates and aggregate constituents. However, the pore space in all cases is only partially filled by nepheline and open and filled pores can be situated right next to each other. The content of nepheline is variable between aggregates. This is partly governed by the pore space provided by the olivine stacks and the aggregate. However, there are also aggregates present which, in spite of their high porosity, contain only small amounts of nepheline.

Sodalite is a rare phase in common aggregates and occurs in much the same way as nepheline.

Clinopyroxene is a rare phase and mostly occurs scattered throughout All-AF, sometimes intergrown with olivine. It also occurs as part of aggregates associated with olivine, sulfides, and metal and occasionally forms rims around small aggregates. Such small clinopyroxene bearing aggregates are usually found in the matrix and are not parts of common silicate-rich aggregates in contrast to isolated crystals.

2.1.2. Principal Types of Silicate-Rich Objects

Silicate-rich objects comprise

1. Isolated fluffy olivine stacks (compare Figures 2 and 4). If large (> 300 μm), they are round and at least partly covered by a dense olivine rim (round objects in Figure 2). They mimic chondrules consisting of a single thinly plated olivine crystal. However, they contain abundant pore space which is only partly filled by nepheline (and no mesostasis). These objects are always very poor in opaque phases. Smaller ones can be angular, show no intergrowth of olivine stacks over the total surface and can be covered by metal. Small olivine stacks (10–20 μm) are abundantly present in the matrix (Figs. 3, 4 and others) and are parts of aggregates.

2. Olivine aggregates consist of fairly large intergrown olivine stacks (200–300 μm) of random orientation. The surface of such aggregates is usually irregular but rounded and covered in places by a dense

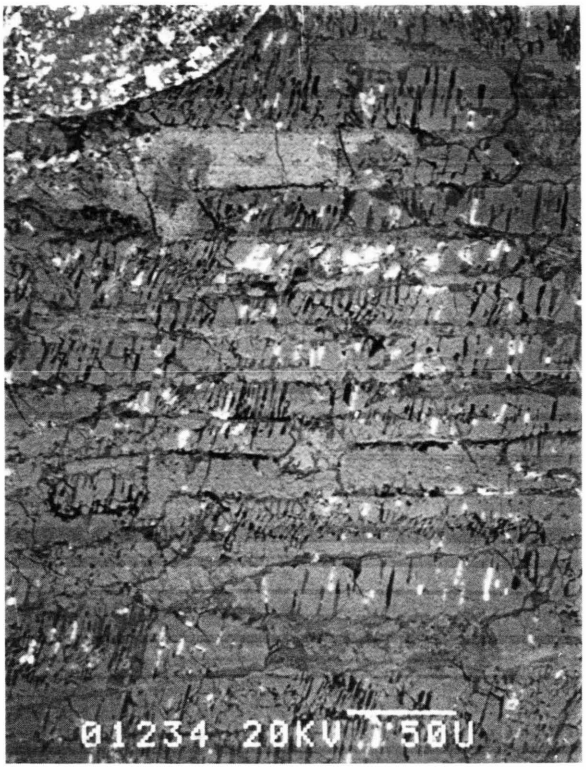

Fig. 5. Barred olivine (from large complex aggregate AF-9) consisting of stacks of olivine platelets which are stapled perpendicular to the bars (thick plates). The large plates are separated from each other by nepheline and fine-grained (<1 μm) mixtures of olivine and andradite. The lighter grey bar near the upper end appears to be a replacement of olivine by a mixture of olivine and andradite. In the left upper corner a portion of an oval silicate-sulfide-metal aggregate is visible. BSE picture. Length of picture is 340 μm.

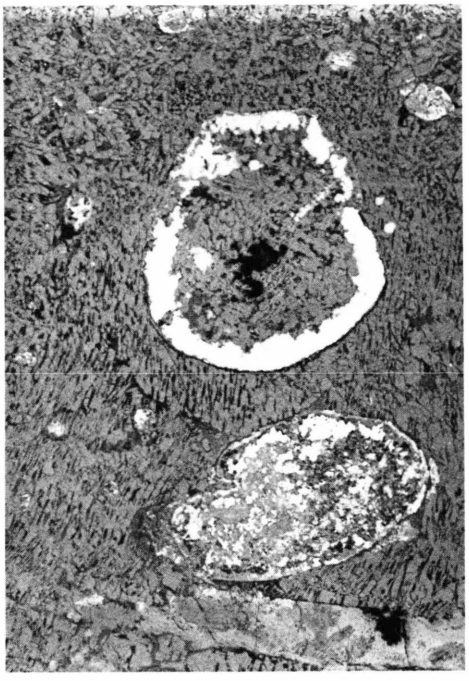

Fig. 7. Two types of silicate-sulfide-metal objects in complex aggregate AF-9. The one in the center consists of an aggregate of olivine stacks with interstitial nepheline partially intruded and covered by sulfide and metal (the large dark holes stem from sputtering with an ion microprobe). The olivine of this object has a brownish-yellow color and is very rich in Cr_2O_3 and Al_2O_3 (compare Table 1). The other object is typical for the most common silicate-sulfide-metal aggregates. BSE picture, length is 450 μm.

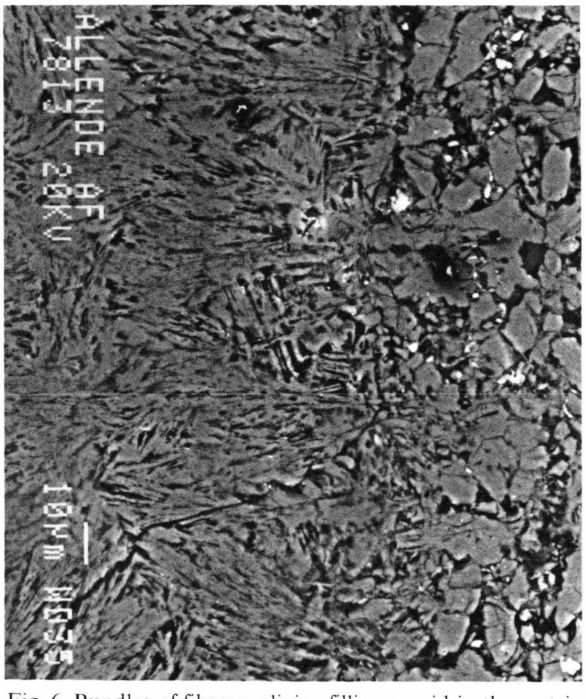

Fig. 6. Bundles of fibrous olivine filling a void in the matrix of All-AF. Similar fibrous olivines fill also cracks (compare Figure 2). Secondary electron (SE) picture, length is 180 μm.

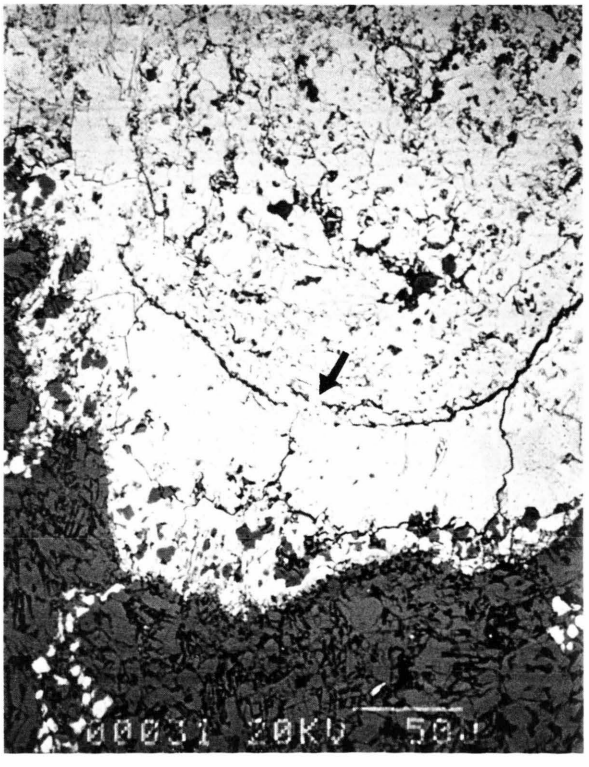

Fig. 8. Portion of a sulfide-rich nodule from a silicate-rich aggregate. The core is rich in fine-grained silicates and phosphates intergrown with troilite. The broad rim consists of massive troilite and pentlandite. Near the core-rim boundary are visible a few refractory metal rich nuggets and HgS (white dots, arrow). BSE picture, length is 330 μm.

olivine shell much like those of the isolated olivine stacks. The pore space is also partly filled by nepheline and the aggregates are also very poor in opaque phases.

3. Complex silicate-rich aggregates (Figs. 1, 2, 9, 10) are the most common objects in Allende-AF. They typically consist of a silicate core consisting either of barred olivine or an intergrowth of fluffy olivine stacks. On top of this is a layer rich in large silicate-sulfide-metal objects which is followed by aggregates of smaller fluffy olivines and sulfide objects. The surface of these objects is commonly decorated by abundant, mostly medium (20 μm) to large (200 μm) sized silicate-sulfide-metal objects (see Figure 10). However, the common olivine stacks grow undisturbed beyond that layer and beyond the outer rim which usually is decorated by medium ($\sim$20 μm) to small ($<$10 μm) sized sulfide-rich objects. Actually, the border between aggregates and the matrix is hardly discernible under the scanning electron microscope because olivine platelets continue to protrude into the matrix in many places. The latter, however, can be distinguished by a fairly chaotic aggregation of, on average, smaller stacks of olivine platelets as compared to that of the silicate-rich aggregates.

4. Aggregates of complex aggregates are rare and form large (up to 2 mm) bodies which tend to be round in spite of the highly irregular lobate forms of their subunits. The subaggregates are mostly separated by matrix-like material. In voids and cracks there is commonly fibrous olivine (Figure 2).

2.2. Exotic Objects

2.2.1. Concentric Olivine-Sulfide-Metal Aggregates (Figure. 11)

Large (100–400 μm) round objects consisting mainly of compact round olivine-sulfide objects. A core of a granular olivine-sulfide-metal intergrowth is surrounded by several layers of round to oval rimmed and rimless olivine-sulfide-metal objects which are embedded in an olivine matrix. This matrix is mostly dense and contains patches of nepheline and little pore space as compared to the silicate-rich aggregates. Some objects have dense sulfide matrices instead of an olivine matrix (Figure 11). The outer rim is made of olivine impregnated by sulfides which at the surface form a thin discontinuous rim. Fairly dense blocky and fluffy olivine covers the whole objects with a tendency for the olivine platelets being oriented perpendicular to the surface.

2.2.2. Sulfide-Andradite Objects (Figure 12)

These are large (up to 5 mm) objects of mostly triangular shape consisting of a massive sulfide core surrounded by a dense intergrowth of coarse-grained andradite, salitic clinopyroxene, olivine, and nepheline. The massive sulfide consists of troilite and pentlandite and contains abundant inlcusions of olivine, andradite, nepheline, phosphate, Ti-magnetite and rare native Cu (Figure 13). Andradite and phosphates develop crystal forms against the sulfide. The dense andradite mantle is commonly surrounded by large (up to 1.5 mm thick) halos consisting of extremely fluffy olivine (very abundant giant plates) and large amounts of interstitial nepheline and pore space (Figure 14). The olivine plates are very large (several mm^2) but thin ($<$10 μm) and commonly bended. They can be solid but more commonly they are hollow, consisting of actually two plates which are partly intergrown with each other. The inner surface is mostly fairly smooth with only few spines protruding into the open space perpendicular to the plate and forming bridges. (The pore space is now mostly filled by nepheline and salite.) The outside surface is very rough and densely covered by spines growing away from the plate up to three plate diameters. The space between the large olivine plates is filled by loosly attached fluffy olivine intergrowths or well intergrown small stacks of olivines with extremely abundant pore space in between. The halo around sulfide-andradite objects includes abundant small, mostly irregularly shaped silicate-rich aggregates.

3. Mineral Compositions

Since almost all objets encountered in All-AF and the rock itself have never been seen before, they need a thorough study by utilizing proper techniques. Here we report on results of a routine chemical characterization of the common phases by making use of a conventional electron microprobe (EMP). However, many phases are very fine-grained and intimately intergrown on a scale which does not in all cases allow clear resolution by the technique applied. Extensive studies utilising a scanning electron microscope have, however, shown that the quantitative analyses obtained with the elec-

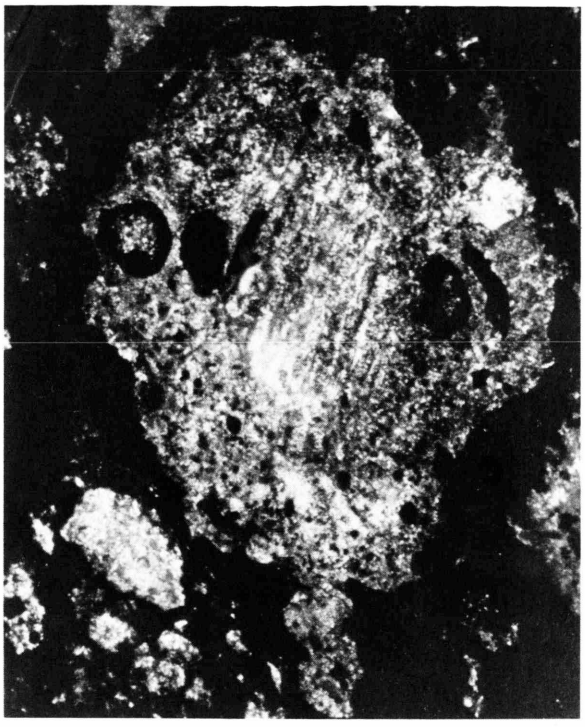

Fig. 9. Complex aggregate (AF-9) with large barred olivine (see Fig. 5) in center covered by a mantle of finer-grained aggregates rich in silicate + sulfide + metal objects (Fig. 7), some of them very large. Note lobate outline of aggregate and small fine-grained aggregates in matrix. Transmitted light picture, length is 1.3 mm.

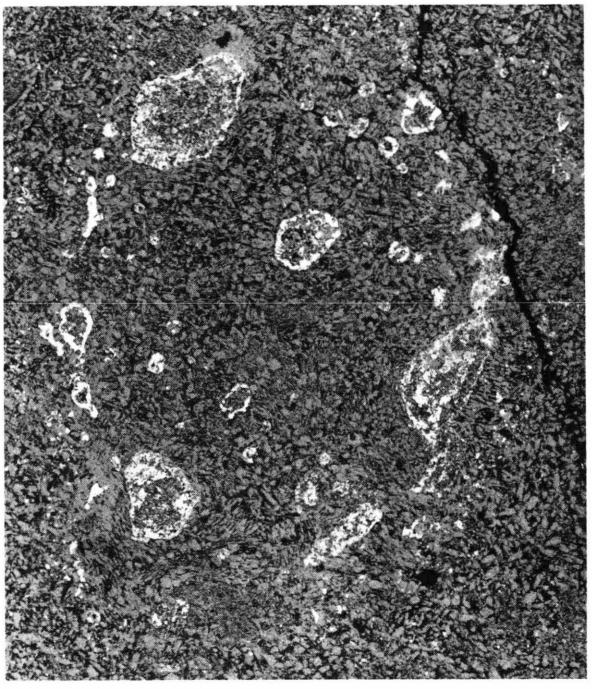

Fig. 10. Complex silicate-rich aggregate consisting of fluffy olivine stacks and complex silicate-sulfide-metal aggregates mostly at the outer part of the main aggregate. The aggregate texture continues into the matrix which differs from the aggregate by the smaller size of olivine stacks, their chaotic arrangement and the greater abundance of small silicate-sulfide objects. BSE picture, length is 870 μm.

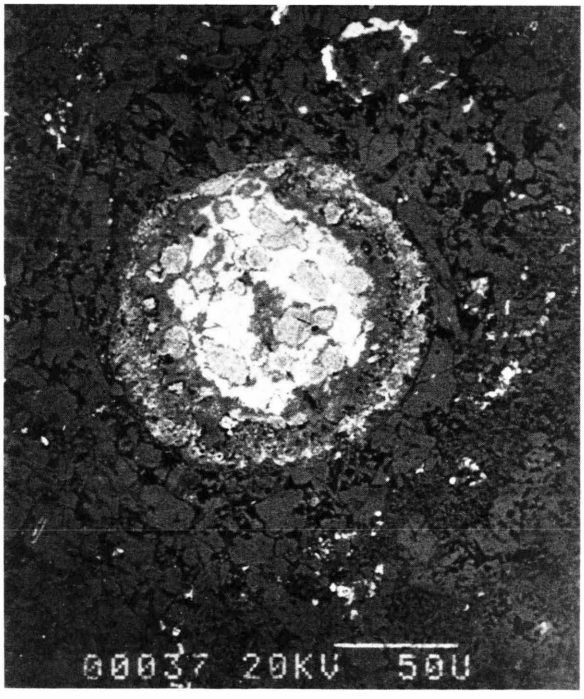

Fig. 11. Concentric sulfide-olivine objects with a core consisting of fluffy olivine stacks and round sulfide-olivine aggregates set into a matrix of dense sulfide and rare metal, covered by a mantle rich in olivine, and an outer rim of olivine + sulfide intergrowths. Note the growth of large olivines at the surface. BSE picture, length is 300 μm.

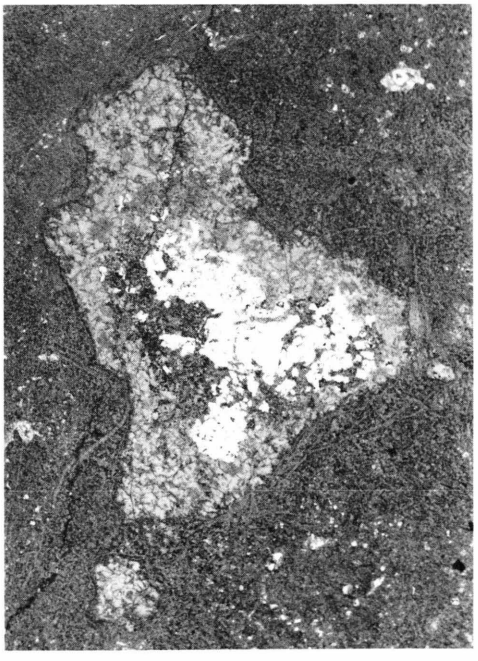

Fig. 12. Sulfide-andradite-olivine object of typical triangular cross-section. The core is massive sulfide (white) surrounded by massive andradite (light grey) and olivine (grey). The dark checkered area inside the object is an intergrowth of nepheline and olivine with minor andradite. The object is surrounded by a highly porous halo which is very rich in large bended olivine plates and interstitial nepheline. BSE picture, length is 4500 μm.

Table 1. Electron microprobe analysis of major silicates in silicate-rich aggregates of All-AF (in wt%). Total Fe given as FeO. Ol = olivine, Cpx = clinopyroxene.

	All-AF-9: Silicate-rich aggregate with BO center							All-AF-5/5: Oval object
	BO center		Off center			Sil.-sulf. objects		
	Ol center	Ol rim	platy Ol	platy Ol	blocky Ol	platy Ol	gran. Ol	fibrous Ol
N	6	2	6	2	2	4	2	3
SiO_2	37.4	38.3	37.5	37.4	37.2	35.8	34.8	35.7
TiO_2	0.10	0.05	0.04	<0.02	0.04	<0.02	0.25	0.02
Al_2O_3	1.20	1.06	0.73	0.46	0.66	2.7	2.9	0.62
Cr_2O_3	0.22	0.13	0.21	0.26	0.17	1.67	2.6	<0.02
FeO	22.6	24.1	26.0	26.3	24.5	23.9	23.8	36.1
MnO	0.20	0.19	0.21	0.22	0.17	0.16	0.16	0.25
NiO	0.07	0.06	0.13	0.15	0.08	0.39	0.23	0.05
MgO	37.3	37.0	35.0	34.9	35.3	34.4	32.1	27.6
CaO	0.21	0.19	0.14	0.15	0.17	0.36	0.66	0.15
Na_2O	0.08	0.10	0.08	0.07	0.30	0.12	0.97	0.08
K_2O	<0.02	<0.02	<0.02	<0.02	<0.02	<0.02	<0.02	<0.02
Total	99.38	101.18	100.04	99.91	98.59	99.50	98.47	100.57

	All-AF-5: Aggregate of silicate-rich aggregates with sulfurized portions						"Matrix"			
	Aggregates				Fibrous object					
	far from sulfides blocky Ol	blocky Ol	Cpx	near sulfides Ol	Ol	Cpx	blocky Ol	blocky Ol	anhedral Ol	Ol
	5	5	2	6	4	1	4	2	2	2
SiO_2	35.4	35.0	54.0	34.6	35.0	52.4	36.9	35.2	37.1	36.0
TiO_2	0.15	0.07	0.93	0.10	0.03	0.24	<0.02	0.09	0.08	0.09
Al_2O_3	1.30	0.88	3.7	1.20	1.69	0.51	0.89	0.81	1.65	1.68
Cr_2O_3	0.49	0.32	0.72	0.42	0.03	<0.02	0.29	0.28	0.07	<0.02
FeO	35.6	37.5	1.39	39.0	38.4	12.8	25.1	31.0	26.0	26.4
MnO	0.21	0.23	0.22	0.26	0.26	0.19	0.21	0.24	0.26	0.30
NiO	0.18	0.43	0.07	0.09	<0.02	<0.02	0.09	0.60	0.19	<0.02
MgO	27.2	25.1	19.4	24.2	23.9	11.7	34.1	29.7	33.1	34.0
CaO	0.20	0.20	20.8	0.19	0.17	22.6	0.28	0.28	0.40	0.42
Na_2O	0.18	0.06	0.05	0.09	0.06	0.02	0.25	0.07	0.10	0.09
K_2O	<0.02	<0.02	<0.02	<0.02	<0.02	<0.02	<0.02	<0.02	<0.02	<0.02
Total	100.91	99.79	101.28	100.15	99.54	100.46	98.11	98.27	98.95	98.98

tron microprobe are representative of the phases present. Averaged and selected analyses of the major minerals of All-AF are given in Tables 1–3.

3.1. Olivine

Olivine of All-AF is rich in FeO with a range from 22.0 to 40.5 wt% (%Fa 25–50) (Figure 15). Contents of FeO vary within larger single stacks of platelets and BO structures and within a given aggregate. The range, however, is restricted and amounts to up to 4 wt% FeO within an aggregate (compare All-AF-9 in Table 1). Olivines from different aggregates apparently have different mean FeO contents and variable ranges thereof.

Minor element contents are unusually high. TiO_2 contents are mostly above 0.05 wt% and can range above 0.2 wt%. Al_2O_3 contents are mostly between 0.5 and 1.8 wt% and can reach almost 3 wt%. Cr_2O_3 contents are commonly between 0.2 and 0.6 wt% and can also reach up to over 2.5 wt%. Contents of CaO are always above 0.1 wt% and range up to over

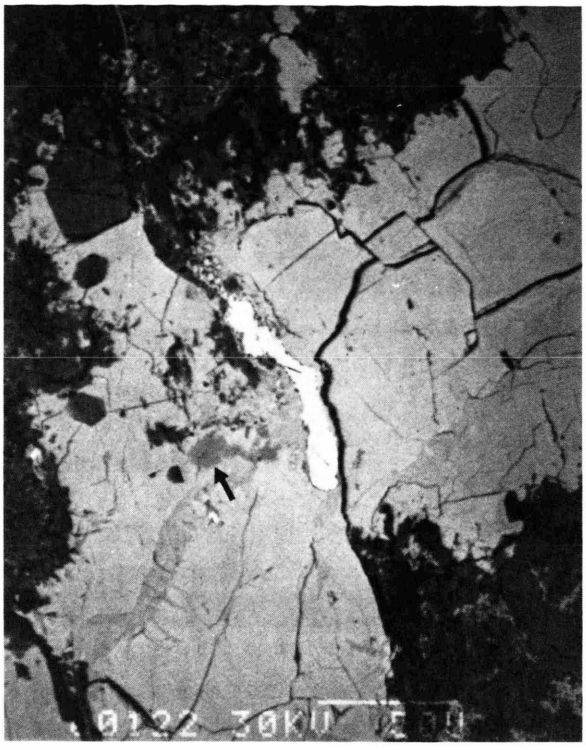

Fig. 13. Massive sulfide core of a sulfide-andradite object showing sulfides (light-grey), native Cu (white), Ti-magnetite (grey, arrow) and silicates and phosphates (dark grey). Note the euhedral shapes of andradite included in sulfide. BSE picture, length is 270 μm.

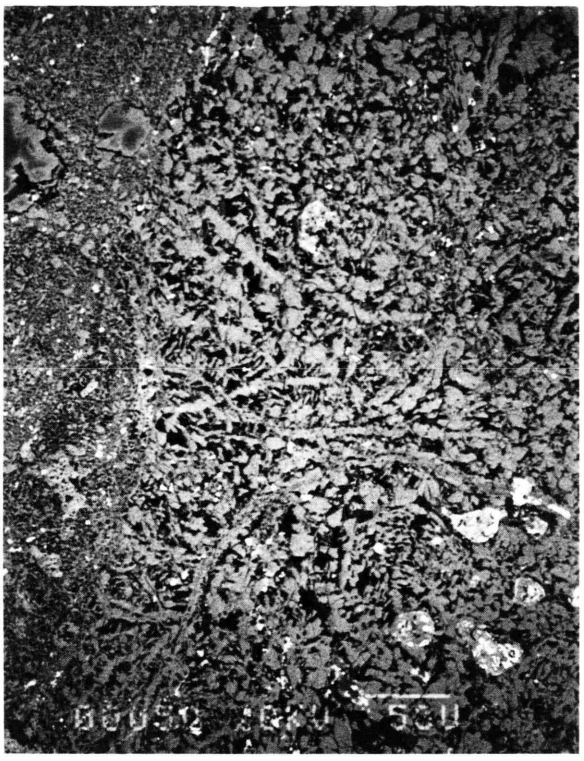

Fig. 14. Portion of matrix of Allende fragment AF which is rich in large bended olivine plates and which borders to normal Allende matrix at the left. Note the abundant pore space (black) and the development of dendritic olivines in large pores. Part of the pores are filled by nepheline. BSE picture. Length is 430 μm.

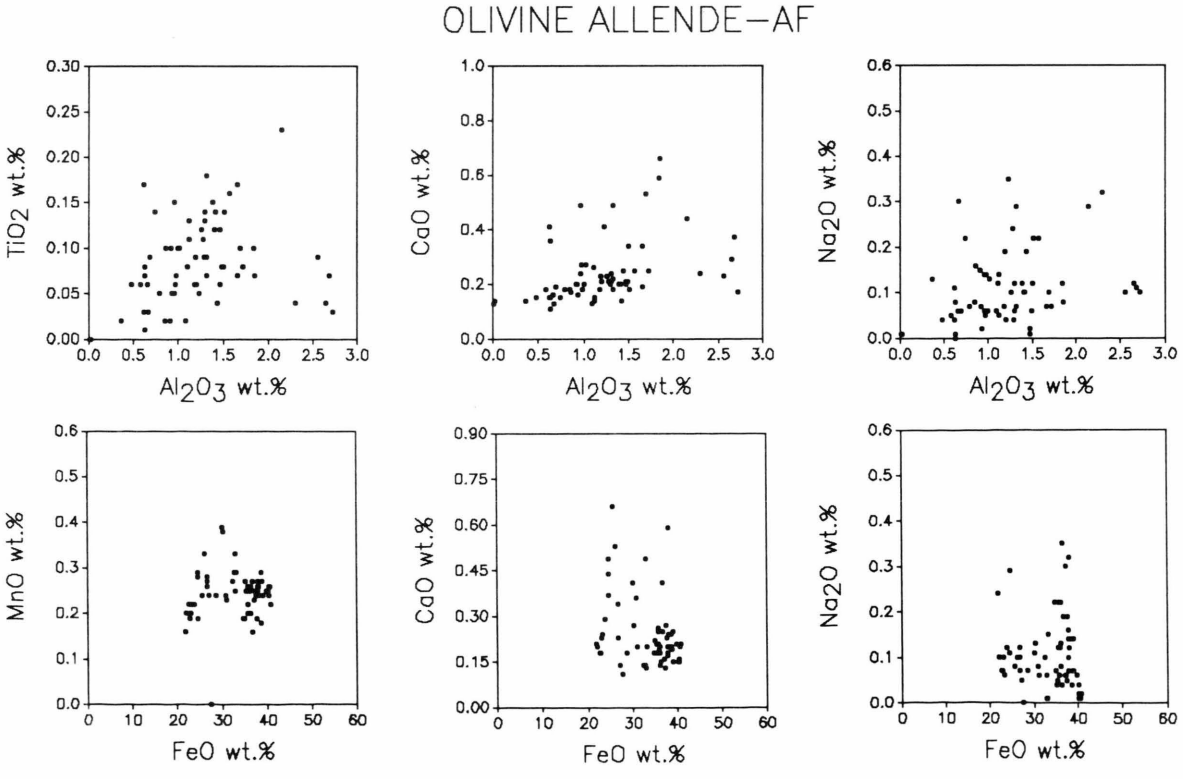

Fig. 15. Minor element contents of olivine of All-AF. Plots of wt% TiO_2, CaO, and Na_2O versus wt% Al_2O_3 and wt% MnO, CaO, and Na_2O versus wt% FeO.

Table 2. Electron microprobe analyses of major phases in sulfide-andradite objects (in wt%). Fe is given as FeO, except for andradite (Fe_2O_3 calculated). Ol = olivine, Andr = andradite, Cpx = clinopyroxene, Ti-mt = titanomagnetite, Per = perovskite. * includes 0.54 wt% V_2O_3. + includes 0.20 wt% V_2O_3.

	All-AF-2: Sulf.-andr. object				All-AF-13: Sulf.-andr. object						All-AF-17: sulf.-sil.-met.-aggr.	
	In sulfide		Andr. mantle		In sulfide		Andr. mantle			"Rim"	Matrix	Surface
N	Ol 2	Andr 2	Andr 4	Cpx 1	Andr 1	Ti-mt 12	Andr 1	Ol 4	Per 9	Cpx 1	Ol 1	Ol 1
SiO_2	35.1	35.6	36.1	35.5	35.0	–	36.2	36.3	0.20	45.1	33.9	34.8
TiO_2	0.05	0.05	0.09	10.2	0.21	26.3	0.07	0.09	57.0	3.0	0.02	0.15
Al_2O_3	0.96	1.27	1.40	20.0	1.18	1.90	1.14	1.70	0.29	4.5	0.91	0.96
Cr_2O_3	<0.02	<0.02	0.04	0.07	<0.02	0.04	<0.02	0.13	<0.02	0.06	1.96	0.57
Fe_2O_3	–	28.0	26.7	–	32.2	16.6	27.3	–	–	–	–	–
FeO	38.7	1.15	1.10	2.29	0.05	54.0	1.36	25.4	0.70	11.8	33.1	32.9
MnO	0.18	<0.02	0.03	<0.02	<0.02	0.54	0.04	0.30	<0.02	0.27	0.29	0.25
NiO	0.02	<0.02	<0.02	<0.02	<0.02	<0.02	<0.02	<0.02	<0.02	0.06	0.96	0.46
MgO	22.9	0.03	0.05	7.4	0.11	1.13	0.06	34.5	<0.02	13.1	26.9	28.1
CaO	0.24	32.3	32.7	24.7	32.6	0.55	32.7	0.45	41.0	22.0	0.20	0.49
Na_2O	0.14	<0.02	<0.02	0.08	0.09	<0.02	<0.02	0.09	<0.02	0.22	0.15	0.06
K_2O	<0.02	<0.02	<0.02	<0.02	<0.02	<0.02	<0.02	<0.02	<0.02	<0.02	<0.05	<0.02
Total	98.29	98.40	98.21	100.24	101.44	101.60*	98.87	98.96	99.43+	100.11	98.39	98.74

Table 3. Electron microprobe analyses of opaque phases in different objects of All-AF (in wt%). Pent = pentlandite, Aw = awaruite, Tr = troilite.

	Silicate-rich aggregates				Sulf.-andradite objects	
	Sil.-sulf.-met. aggregate (ring structure)		Massive sulf. nodule			
	Pent	Aw	Pent	Tr	Pent	Tr
Fe	42.3	29.8	47.4	63.3	44.9	63.2
Co	1.57	2.12	1.0	0.10	1.68	0.09
Ni	22.0	68.8	18.0	0.17	20.4	<0.02
Si	0.19	0.10	0.55	0.02	<0.02	<0.02
Cr	0.06	0.05	0.05	0.08	<0.02	<0.02
P	0.36	0.20	<0.02	0.32	<0.02	<0.02
S	32.5	0.06	32.9	34.7	31.5	36.1
Total	98.98	101.13	99.90	98.69	98.48	99.39

0.5 wt%. Contents of MnO range between 0.16 to 0.4 wt%. Practically all olivines of All-AF contain Na_2O, mostly between 0.05 to 0.15 wt% with a range up to over 0.3 wt%. Most analyses show the presence of NiO with a wide range between <0.02 wt% and about 1 wt% and a cluster between 0.05 and 0.5 wt%.

There is virtually no correlation between any pair of major and/or minor elements (Figure 15). Exceptions could possibly be the refractory elements Ti, Al, and Ca. If a few Al- (and Cr-) rich olivines are excluded, a fair positive correlation between TiO_2 and Al_2O_3 becomes visible, a weak one for CaO and Al_2O_3. No hint of a correlation is visible for pairs of medium volatile and volatile elements, not even for MnO vs. FeO.

Analysis by ion microprobe spectrometry [29] revealed that All-AF olivines are also rich in refractory lithophile elements with rare earth element abundances around 1 × CI and Be, Zr, and Nb enriched between 3–5 × CI abundances.

3.2. *Pyroxenes*

Aluminous diopsides present in aggregates and in the matrix (compare All-AF-5 in Table 1) contain typically about 3–4 wt% Al_2O_3, about 1 wt% TiO_2, and between 0.5 and 1 wt% Cr_2O_3. They are poor in FeO (mostly between 1–1.5 wt%) but always contain appreciable amounts of MnO (0.2–0.3 wt%).

Salites are associated with fibrous olivines (compare analyses from All-AF-5 in Table 1), are poor in TiO_2 (0.2–0.3 wt%) and Al_2O_3 (approx. 0.5 wt%) and contain between 11 and 13 wt% FeO. Their FeO/MgO ratios are comparable to the average FeO/MgO ratio of the olivines.

Highly aluminous and titaniferous clinopyroxene of the sulfide-andradite objects (se All-AF-2 in Table 2) is poor in Cr_2O_3 (<0.1 wt%), FeO (approx. 2 wt%, and MnO (<0.02 wt%).

In discontinuous rims around the massive andradite mantle of sulfide-andradite objects there is present a titaniferous augite (see All-AF-13 in Table 2) which has variable but fairly high contents of TiO_2 (2–5 wt%) and Al_2O_3 (3–6 wt%), FeO (11–13 wt%) and MnO (0.25–0.3 wt%).

3.3. *Nepheline*

Nepheline ($NaAlSiO_4$) has a fairly uniform composition except for elements usually not present in appreciable amounts. Contents of K_2O are typically between 1.5 and 2 wt%, CaO between 2 and 2.5 wt% and the Na/K ratio is close to 9 (primitive).

3.4. *Troilite*

Troilite (FeS) (Table 3) is commonly poor in minor elements but always contains some Co (around 0.1 wt%). It sometimes appears to contain also small amounts of Ni, Si, Cr, and P.

3.5. *Pentlandite*

Pentlandite, $(Fe, Ni)_9S_8$, (Table 3) contains usually between 17 to 22 wt% Ni. The high-Ni pentlandite coexists with awaruite. Cobalt contents are around 1.6 wt% and common are small contents of Si, Cr, and P.

3.6. *Awaruite*

Awaruite is the only metal phase present and contains about 69 wt% Ni, 2.1 wt% Co and minor amounts of Si, Cr, and P.

3.7. *Accessory Phases*

There is a large variety of mostly rare accessory phases present in All-AF, the exact composition and nature of which could not be determined in the course of the routine investigation. A summary of the phases found and their principal occurrences is given in Table 4. Noteworthy is the wide-spread occurrence of platinum-group-element (PGE) nuggets. They are present throughout All-AF and are most commonly associated with sulfides with the exception of sulfide-andradite objects where they occur associated with silicates. Surprising is also the presence and abundance of HgS which was found in massive sulfide nodules of silicate-rich aggregates and associated with PGE nuggets in andradite of sulfide-andradite objects. Phosphates (whitlockite and apatite?) are also fairly common and always associated with sulfides.

Table 4. Accessory phases tentatively identified in All-AF.

Phase	Occurence	Composition
(A) *Common silicate-rich aggregates*		
PGE nuggets	Olivine-sulfide objects	Pt-Ir-rich
HgS	Massive sulfide	
Ca-phosphate	Massive sulfide	Na-bearing
(B) *Concentric olivine-sulfide-metal aggregates*		
PGE nuggets	Olivine-sulfide objects	Pt-Ir-rich Multiphase (Pt, Os)
(C) *Sulfide-andradite objects*		
Cu	With pentlandite and troilite	2–5 wt% Fe
PGE nuggets	In andradite	Os-Ru-rich
	In andradite	Pt-Ir-rich
	In andradite	Multiphase
HgS	In andradite-olivine intergrowths (veins) with PGE nuggets	
Ti-magnetite	In sulfide and andradite	
Ilmenite(?)	Rims around perovskite in andradite	
Perovskite	In andradite-olivine mantle	Some FeO-bearing
Ca-phosphate	In sulfide	Na-bearing
Barite	In andradite-olivine mantle	
Calcite	Associated with barite	

The exotic sulfide-andradite objects contain the most exotic accessoires: Beside those mentioned above they contain native Cu and Ti-magnetite (associated with the sulfides), ilmenite, perovskite and barite associated with andradite and olivine. One grain was encountered which gave only a Ca signal of the right proportion to be tentatively identified as being probably calcite.

One reviewer was concerned that some of the rare phases may have been introduced during sample handling. We believe this to be unlikely because All-AF was treated in exactly the same way as chondrules (e.g. [30]), dark inclusions (e.g. [19]) and other meteoritic lithologies utilizing identical tools. None of these samples contained any of the exotic phases encountered in All-AF.

4. Discussion

4.1. Olivine Morphologies

Olivine morphologies are highly anisotopic and indicative of growth from a vapor phase (e.g. [31]). This view receives strong support by the high minor and trace element contents and the high porosity of the olivines which make an igneous origin very unlikely. The typical and wide-spread growth form are stacks of thin (5–10 μm) olivine plates. It is the principal form of olivines in All-AF and it is a wide-spread relictic form in all chondrites. The stacks of platelets can – in the course of continuing condensation – grow together and ultimately form solid olivine crystals. This is commonly the case with small stacks in All-AF but could possibly affect larger ones in other meteorites.

Intergrown olivine stacks can also form larger olivine plates the shape of which are oriented perpendicular to the orientation of the original platelets. The "barred" olivine (BO) structure formed this way is present in all chondrites (and in Bencubbin) implying a similar genesis of at least a portion of these objects. The different types of olivines apparently reflect diffent growth conditions. From the type of occurrence of morphologically different olivines we can establish a time-sequence which probably also reflects changing conditions. The BO structure (Fig. 5) exclusively occurs inside and near the center of silicate rich aggregates. Presumably it is the earliest type of olivine growing from a vapor. The BO structure was apparently followed by large stacks of olivine platelets (see e.g. Fig. 7). These are either part of silicate rich complex aggregates or form objects of their own (Figs. 2 and 4). Stacks consisting of gradually smaller numbers of platelets are parts of complex aggregates or of the matrix. Fibrous olivines fill cracks and voids and therefore apparently are the latest condensates to form. This morphological sequence seems to reflect changing conditions with time with the BO structure reflecting high oversaturation and undercooling (and hence high growth rate). The following morphological types of olivines could have formed under conditions of decreasing oversaturation and undercooling, analogous to the formation of ice crystals in the terrestrial atmosphere (e.g. [31]).

The very large bended plates of olivine (Fig. 14) associated with sulfide-andradite objects cannot easily be placed among the sequence outlined above because they do not take part in aggregate formation. They have dimensions exceeding those of the common aggregates signalling high growth rates and low gas dynamics.

4.2. Chemical Composition of Olivine

The olivine stacks and the huge bended olivine plates with dendritic growth features at their surface make the conclusion inescapable that they grew from the vapor phase. The generally high and sometimes very high minor element (Al, Ca, Ti, Cr) and trace element (e.g. REE) contents of the olivines strongly support this view. These minor element contents exceed those of olivines in carbonaceous chondrites [4], [32–38] and ureilites [39–42]. The high and correlated abundances of the refractory elements Ti and Al are compatible with a condensation origin of the All-AF olivines. The low olivine-liquid distribution coefficients for these elements [43, 44] and the lack of any identifyable melt in All-AF make an igneous origin of the olivines of All-AF very unlikely.

The third refractory element present in appreciable amounts in All-AF olivines, Ca, does not show a correlation with Ti and Al comparable to that observed for isolated olivines in carbonaceous chondrites (e.g. [36–38]). This lack of Ca-X correlations could be accounted for by the recent discovery of the highly volatile character of Ca under oxidizing conditions due to the formation of $Ca(OH)_2$ [45, 46]. Thus, the FeO-poor (reduced) isolated olivines retained their Ca-Al and Ca-Ti correlations whereas the FeO-rich olivines of All-AF apparently have re-equilibrated CaO contents. They cluster around 0.2 wt% CaO and appear to be buffered by an oxidizing environment. Therefore, CaO contents of All-AF olivines are lower than that of isolated olivines in carbonaceous chondrites. Also Ti and especially Al contents appear to be slightly disturbed, probably by post-condensation mobilization processes [29].

The moderately volatile elements show clusters comparable to that of Ca: Cr_2O_3 around 0.4 wt%, MnO around 0.23 wt%, and Na_2O around 0.08 wt%. The lack of any correlation between them could be taken as an indication of an attempted equilibration with the local gas phase. That would imply exchange processes with the vapor phase [30], [47–49].

The FeO contents of olivines apparently reflect the very same process and it appears that the majority of

olivines aquired its FeO by a metasomatic exchange reaction with the vapor phase. The range and the average FeO content of olivines of a given aggregate are smaller and different, respectively, from the bulk. This could indicate separate histories for the individual aggregates and different grades of "equilibrium" attained with the vapor phase. Olivine FeO contents are roughly correlated with their position within a given aggregate (compare All-AF-9 in Table 1) with the FeO-poor compositions present in the core. We take this as a strong indication that metasomatism of the olivines took place when the aggregates already existed.

The FeO-rich olivines are commonly associated with sulfide-rich objects. These olivines have the highest FeO/MnO ratio. Apparently, they did receive the Fe^{2+} not only from the vapor, which should produce an Fe-Mn correlation, but also from locally oxidized metal similar to what has been described from olivines in normal Allende [50]. The second type of FeO-rich olivine is the fibrous olivine that fills voids and cracks. This setting indicates that the fibrous olivines must have formed late in the history of All-AF, after the rock accreted. Since their chemical compositions are consistently FeO-rich, it appears likely that they formed by condensation from a common, highly oxidized reservoir. This view is supported by the composition of occasionally co-existing clinopyroxenes (Table 1). They are FeO-rich and apparently close to equilibrium with olivine with respect to the Fe-Mg distribution (see below). Apparently, vapor-solid exchange reactions and redeposition of matter via the vapor phase continued after accretion of aggregates into a rock (the size of which remains unknown).

The olivines encountered in a silicate-sulfide-metal object inside aggregate All-AF-9 (Table 1) have very unusual compositions in being very rich in Al and Cr. The Al content could be primary and the Cr locally derived from oxidized metal, but the low Ti contents do not fit that picture. There are two possible explanations for this: (1) These olivines condensed after most of the Ti was extracted from the vapor phase, or (2) Ti was mobilized and lost during subsequent metasomatic exchange reactions. Why it did so in this case and not in the others is, however, not clear. In any case, the concerted enrichment of Al and Cr apparently is due to the very same process: enrichment from a vapor, which could have been locally strongly oversaturated in both elements.

4.3. Chemical Composition of Clinopyroxene

Calcium-rich clinopyroxene is the only pyroxene present in All-AF. This is highly unusual for a chondritic rock. In fact, All-AF is the only example sofar. Apparently the constituents of All-AF escaped a common process in the solar nebula, namely the conversion of parts of the primary olivines into low-Ca pyroxenes by reaction with the vapor phase (see [49]).

The most common clinopyroxene, aluminous diopside, is always associated with olivine, either intergrown or – rarely – forming rims around small olivine-clinopyroxene aggregates. This diopside is the only silicate phase within All-AF which has a low FeO/MgO ratio outside the range of all others and especially that of the olivines. We interpret this low ratio as relictic and being due to the low diffusion rates for Fe^{2+} and Mg^{2+} in clinopyroxene as compared to olivine [51, 52]. In the previous section we discussed formation of FeO-rich olivine as a result of attempted equilibration of forsterite with the ambient FeO-rich gas. The time span for this process apparently was too short and the temperature too low to affect clinopyroxene with its much lower diffusion coefficient for Fe^{2+}. The coexistence of FeO-poor pyroxene with fayalitic olivine is common in Allende. Presence of diopsides thus demonstrates that the original composition of the minerals in All-AF must have been poor in Fe^{2+}. It can therefore be assumed that most major phases of All-AF originally grew in a reducing environment. Consequently, the FeO now present in all phases is very likely to be mainly of secondary origin and due to a metasomatic exchange reaction between pre-existing Fe-poor solids and an oxidized vapor phase.

The salites coexisting with fibrous olivine could be later condensates – as can be judged from their much lower contents of TiO_2 and Al_2O_3. Since fibrous olivines mostly fill voids and cracks they must be very late local condensates, preferentially utilizing the given pore space [53]. If this is so, the salites which are intimately intergrown with the fibrous olivine, must have a very similar origin. The low abundances of refractory elements are in agreement with this mechanism.

Iron-rich clinopyroxene is also encountered in discontinuous rims covering complex silicate-rich aggregates and the fragment All-AF itself. Rim formation occurred continuously during aggregation, accretion, and after break-up of the accreted rock before incor-

poration into the Allende meteorite. This could have taken place via a vapor phase which tried to escape the object in question but apparently upon contact with the ambient vapor precipitated clinopyroxene at the surface of the object (sort of sweating). The enriched vapor could have been produced by mobilization of the "refractory" element Ca [45, 46] within the object and precipitation at the surface in contact with the ambient vapor (which could have provided most of the other elements).

A FeO-poor clinopyroxene with very high Ti and Al contents is also present in sulfide-andradite objects. This suggests (as do other observations – see below) that it has a relicitic composition which apparently indicates that the sufilde-andradite objects are somehow related to Ca, Al-rich inclusions (CAIs).

4.4. Nepheline

Nepheline is the major alkali-bearing phase. Although some trace amounts of sodalite are present in All-AF and some Na apparently resides in olivines, the Na/K ratio of nepheline is similar to the CI ratio. Since nepheline partially fills the pore space of olivine stacks and aggregates it can only have been deposited from a vapor phase. This condensation will utilize the pore space because it provides cold-traps according to the mechanism of Arrhenius and De [53]. Thus, it appears to be very likely that nepheline condensed directly from the vapor phase into the pore space of olivines and aggregates thereof. If this is so, then Al was either still present in the vapor in sufficient quantity or was mobilized from pre-condensed solids. The very high abundance of nepheline in halos around sulfide-andradite objects (which may represent altered CAIs) suggest a local supply of Al which could have led to the preferential precipitation of nepheline around these objects.

Nepheline associated with olivine of the common silicate-rich aggregates may have formed by reaction of Na with Al provided either by olivine or by volatile Al-species in the vapor.

4.5. Aggregation and Condensation

All-AF aggregates consist of olivine stacks of different orientation and of silicate-sulfide-metal objects. All these constituents are intergrown with each other without change in the principal growth form of olivine. Growth of the original olivine stacks appears to continue during and after incorporation of silicate-sulfid-metal objets. For example, in Fig. 7, the growth of olivine stacks to which such an aggregate has been attached continues undisturbed and envelops the captured object. Thus, aggregation and growth of olivines must have been contemperaneous.

Large complex aggregates of aggregates manifest that olivine growth continued up to a very late stage of aggregation since they are held together by partly intergrown smaller olivine stacks or have larger voids filled by fibrous olivine. The same holds for the whole All-AF fragment which has a compact structure and the matrix of which shows very late growth of fibrous olivines filling voids and cracks (Fig. 2). Although the latter observation gives clear evidence for late olivine growth during accretion it is not clear wether this growth can be directly related to the original gas phase. It is possible that this sort of late olivine growth might be due to internal redistribution utilizing a gas phase as vehicle for mass transport.

4.6. Aggregates and the Formation of Chondrules

Large complex aggregates typical of All-AF are not found in normal Allende. However, sintering, recrystallization and partial melting could transform All-AF aggregates into typical coarse-grained Allende components such as chondrules and recrystallized aggregates. During such a process the fluffy olivine stacks will transform into single, well crystallized olivines. Nepheline will react with olivine to form a partial melt which could be chilled or could crystallize to form a dense matrix as it is observed in recrystallized aggregates of normal Allende. A high degree of partial melting or total melting may lead to formation of real chondrules. This scenario can easily account for textural and chemical properties of chondrules and aggregates of all chondrites, the typical components of which are recrystallized and/or partially molten aggregates. Their individual chemistries reflect mixing of various components in different proportions (e.g. [54]). This is exactly what can be seen in All-AF aggregates: The chemical composition of aggregates in All-AF is determined by mixing of three components – olivine, nepheline, and metal-silicate aggregates. Considering the possibility of a fourth phase taking part in the mixing process (pyroxene) the whole mixing spectrum observed in chondrules of carbonaceous and ordinary chondrites can easily be

explained. This picture implies that chondrule formation occurred before incorporation of FeO into silicates.

Because All-AF aggregates have not been subject to sintering or melting, the original texture formed by aggregation and simultaneous condensation can be studied. Under such conditions coherent aggregates can be formed which do not need an additional glueing agent. Sticking and consolidation is simply achieved by continuing growth of aggregate constituents (mainly olivine) and subsequent pore-filling condensates (mainly nepheline). Efficient sticking not only is of crucial importance for the formation of aggregates in a dynamic environment but also for the survival of these aggregates during subsequent processing such as sintering. Thus, we believe that All-AF provides a clue for the formation of aggregates, the protoliths of chondrules.

4.7. Sulfide-Andradite Objects

The Ca- (andradite) and Al- (nepheline) rich nature of sulfide-andradite objects plus the presence of ilmenite and Ti-magnetite and relictic perovskite, fassaite and PGE nuggets suggest that they represent former CAIs which experienced extensive alteration by reaction with a gas phase at low temperature. Ironically, andradite is the only silicate phase in All-AF which is, in most cases, well crystallized forming large (<100 μm), sometimes euhedral crystals. However, the precursor of these objects must have had a peculiar composition consisting of a metal core surrounded by refractory oxide phases. The metal subsequently was sulfurized and the oxide phases converted into andradite, ilmenite and Ti-magnetite by oxidation and Fe-metasomatism. Unfortunately, no such CAI, consisting of a metal core and a refractory rim, is known and it is not easy to envision the formation of such an object. The shape of the objects might provide a clue. They display predominantly triangular outlines in thin sections (Fig. 12). This implies that their three-dimensional shape might have been tetrahedral. If these tetrahedra were hollow they could have provided the space for metal to condense and fill the cavity similar to what has been proposed for metal-rich CAIs from Efremovka [55]. The distribution of refractory metal rich nuggets in sulfide-andradite objects indicates that the pre-sulfide metal apparently was poor in refractory siderophile elements (because sulfide does not contain PGE nuggets but contains large amounts of the volatile element Cu) and the silicate portion was and is rich in such elements. This could indicate that the silicate portion of these objects originally had CAI composition which was metasomatically altered. This alteration under highly oxidizing conditions (formation of andradite) did not affect the stable PGE nuggets. That view is supported by the presence of relictic perovskite in sulfide-andradite objects and reaction products thereof with oxidized Fe (ilmenite, Ti-magnetite). In addition, the presence of barite in these objects indicates a high abundance of Ba, a refractory lithophile element. Apparently none of the original metal-rich CAIs survived the oxidation and metasomatism event.

4.8. Sulfide-Rich Objects

Sulfides are a common constituent of silicate-sulfide aggregates which are parts of complex silicate-rich aggregates or from aggregates of their own (the concentric olivine-sulfide-metal aggregates). They also occur as massive nodules within silicate-rich aggregates or as massive masses filling voids and cracks mainly in aggregates of aggregates and in sulfide-andradite objects. It appears highly probable that most sulfides now present in All-AF originally were FeNi metal which was sulfurized by the cooling vapor phase. Evidence for sulfurization can be found in large sulfide-rich objects which commonly contain PGE metal nuggets. These nuggets could have been formed by sulfurization of an originally PGE containing metal similar to the process described by [56]. Chemical compositions of the sulfides and the NiFe metal indicate high S and O fugacities and temperatures around or below 250 °C for a final approach towards equilibrium [57, 58]. The Ni content of awaruite in All-AF is similar to that of awaruite in normal Allende [59]. The Co content, however, is significantly higher in All-AF metal which is at the higher end of the variation present in Allende metal.

Compact sulfide-rich nodules apparently are a sulfide-rich version of the ordinary sulfide-silicate-metal objects. Originally they could have consisted of delicate fluffy silicate aggregates embedded in metal. Oxidation of the metal led to formation of phosphates (from dissolved P) and gradual sulfurization could have led to the zonal sulfide distribution with a troilite core and pentlandite-bearing rim. Abundant PGE

nuggets demonstrate the primitive nature of the original metal.

The presence of HgS in sulfides and in between silicates could indicate that either the rock All-AF or the constituents of All-AF were open to vapors down to very low temperatures. The presence of HgS rather than metallic Hg again points towards high S fugacities at low temperatures.

5. Conclusions

All-AF is a chondritic rock with chemical affinities to type 3 carbonaceous chondrites [22, 27]. Its mineralogy and petrography, however, is unique reflecting a unique history. The main constituents of All-AF are silicate-rich, highly porous aggregates consisting of fluffy stacks of olivine platelets, some silicate-sulfide-metal aggregates, and minor nepheline. The morphology and poorly crystalline state of the olivines and their high minor and trace element contents suggest that they formed by condensation from a vapor. No melt or matrix and no low-Ca pyroxenes are present in All-AF. It provides sofar the best sample for the study of condensation and aggregation in space. From our routine examination of All-AF we can arrive at a genetic model which reflects a variety of processes having been active presumably in the solar nebula:

1) Condensation of forsteritic olivines from a vapor under reducing conditions. These olivines form mainly fluffy stacks of crystallographically oriented platelets which are in part intergrown with each other. Condensation of olivine continues through most of the following steps.

2) Condensation of metal into the pore space and at the surface of small aggregates of fluffy olivines (formation of olivine-metal aggregates).

3) Aggregation of fluffy olivine stacks and small but highly variable amounts of olivine-metal aggregates into silicate-rich aggregates of mm size. Growth of olivine continues and leads to intergrowths of the aggregate constituents.

4) Some aggregates aggregate to form aggregates of aggregates. Growth of olivine continues and provides consolidation.

5) Nepheline condenses into the pore space of fluffy olivines and aggregates but utilizes only a fraction of the pore space available.

6) Metal reacts with the vapor and forms sulfides (troilite and pentlandite), awaruite and refractory metal rich nuggets. Either before or during sulfurization.

7) Oxidation of metal takes place leading to formation of phosphates and oxidized Fe.

8) Olivines exchange Mg^{2+} for the Fe^{2+} from the vapor. Individual aggregates are affected to different degrees by this Fe^{2+}-metasomatism. Growth of olivines from the vapor continues (fed by large quantities of Mg liberated from forsteritic olivines).

9) Aggregated and not-aggregated matter and other constituents aggregate into a rock. Olivine continues to grow and leads to intergrowths of the constituents. At this stage olivine is accompanied by salitic pyroxene.

10) Voids and cracks are filled by mobilized sulfides and fibrous olivine.

11) All-AF was broken off a larger piece of rock while redeposition of matter was still going on. The broken surface was thus covered by a discontinuous rind of salitic (hedenbergitic) pyroxene and andradite, apparently a reaction product of vapors from inside the fragment with the ambient gas.

12) The constituents of All-AF missed the high temperature event required for chondrule formation and experienced by aggregates of normal Allende. Therefore, they were exposed much more efficiently to the metasomatizing Fe^{2+}-rich vapor than components of normal Allende. All-AF finally accreted together with the usual components into the Allende parent rock.

Since the bulk composition of All-AF is very similar to that of Allende [22] it is very probable that it was formed within the very same sub-nebula which also produced Allende. However, its constituents and All-AF itself were processed in quite a different way from the normal constituents of Allende. A turbulent sub-nebula could provide the necessary environment which is also required for the aggregates to form.

The comparable sizes of aggregates in All-AF and normal Allende suggest processing under similar physical conditions in a dynamic environment. The total lack of chondrite matrix in All-AF probably indicates an untimely aggregation of the aggregates. As a sizeable chunk it could have survived the high temperature event experienced by the aggregates of normal Allende. However, the high degree of Fe^{2+} metasomatism experienced by All-AF (it is an almost "equilibrated" chondrite) clearly is counterindicative to such a model. This problem, which All-AF shares with ordinary chondrites has to await further studies as do other unresolved questions.

Acknowledgements

This study has been financially supported by the Austrian Fonds zur Förderung der wissenschaftlichen Forschung (project P 5554, G.K., P.I.). We thank Drs. Kurt Fredriksson and Addi Bischoff for constructive reviews.

[1] G. Mueller, Nature London **210,** 151 (1966).
[2] R. S. Clarke, E. Jarosewich, B. Mason, M. Gomez, and J. R. Hyde, Smithson. Contrib. Earth Sci. **5** (1970).
[3] L. A. Fuchs, E. Olsen, and K. J. Jensen, Smithson. Contrib. Earth Sci. **10** (1973).
[4] G. Kurat, Tschermaks Min. Petr. Mitt. **22,** 38 (1975).
[5] R. M. Fruland, E. A. King, and D. S. McKay, Proc. Lunar Planet. Sci. Conf. **9,** 1305 (1978).
[6] A. Kracher, K. Keil, G. W. Kallemeyn, J. T. Wasson, R. N. Clayton, and G. I. Huss, J. Geophys. Res., Proc. Lunar Planet. Sci. Conf. 16th **90,** D123 (1985).
[7] W. R. VanSchmus, Geochim. Cosmochim. Acta **31,** 2027 (1967).
[8] K. Fredriksson, E. Jarosewich, and J. Nelen, in: Meteorite Research (P. M. Millman, ed.), Reidel, Dordrecht 1969, p. 155.
[9] G. Kurat, Earth Planet. Sci. Lett. **7,** 317 (1970).
[10] C. A. Leitch and L. Grossman, Meteoritics **12,** 125 (1977).
[11] R. S. Lewis, L. Alaerts, J. Hertogen, M.-J. Janssen, H. Palme, and E. Anders, Geochim. Cosmochim. Acta **43,** 897 (1979).
[12] M. Prinz, M. K. Weisberg, C. E. Nehru, and J. S. Delaney, Meteoritics **22,** 482 (1987).
[13] R. V. Fodor and K. Keil, Geochim. Cosmochim. Acta **40,** 177 (1976).
[14] L. L. Wilkening and R. N. Clayton, Geochim. Cosmochim. Acta **38,** 937 (1974).
[15] J. F. Lovering, in: Researches on Meteorites (C. B. Moore, ed.), J. Wiley & Sons, New York 1962, p. 179.
[16] L. Wilkening, Geochim. Cosmochim. Acta **37,** 1985 (1973).
[17] R. F. Dymek, A. L. Albee, A. A. Chodos, and G. J. Wasserburg, Geochim. Cosmochim. Acta **40,** 1115 (1976).
[18] G. W. Kallemeyn, W. V. Boynton, J. Willis, and J. T. Wasson, Geochim. Cosmochim. Acta **42,** 507 (1978).
[19] A. Bischoff, H. Palme, B. Spettel, R. N. Clayton, and T. K. Mayeda, Lunar Planet. Sci. **19,** 88 (1988).
[20] T. E. Bunch and S. Chang, Lunar Planet. Sci. **14,** 75 (1983).
[21] R. N. Clayton, N. Onuma, Y. Ikeda, T. K. Mayeda, I. D. Hutcheon, E. J. Olsen, and C. Molini-Velsko, in: Chondrules and Their Origins (E. A. King, ed.), Lunar Planet. Inst., Houston 1983, p. 37.
[22] H. Palme, G. Kurat, B. Spettel, and A. Burghele, Z. Naturforsch. **44 a,** 1005 (1989).
[23] U. Ott, S. Chang, and T. Bunch, Lunar Planet. Sci. **10,** 952 (1979).
[24] J. F. Kerridge, Geochim. Cosmochim. Acta **39,** 1707 (1985).
[25] D. Heymann, C. C. A. H. Van der Stap, R. N. Vis, and H. Verheul, Meteoritics **22,** 3 (1987).
[26] T. E. Bunch, S. Chang, and U. Ott, Lunar Planet. Sci. **11,** 119 (1980).
[27] H. Palme, G. Kurat, F. Brandstätter, A. Burghele, J. Huth, B. Spettel, and F. Wlotzka, Lunar Planet. Sci. **16,** 645 (1985).
[28] G. Kurat, H. Palme, F. Brandstätter, and H. Huth, Lunar Planet. Sci. **18,** 523 (1987).
[29] G. Kurat, E. Zinner, and H. Palme, 52nd Ann. Meeting Meteorit. Soc. Vienna 1989, p. 124.
[30] G. Kurat, H. Palme, F. Brandstätter, B. Spettel, and V. P. Perelygin, Lunar Planet. Sci. **16,** 471 (1985).
[31] E. I. Givargizov, Highly Anisotropic Crystals, D. Reidel, Dordrecht 1987.
[32] G. Hoinkes and G. Kurat, Meteoritics **10,** 416 (1975).
[33] G. Kurat and A. Kracher, Meteoritics **10,** 432 (1975).
[34] H. Y. McSween Jr., Geochim. Cosmochim. Acta **41,** 411 (1977).
[35] A. S. Kornacki and J. A. Wood, Geochim. Cosmochim. Acta **48,** 1663 (1984).
[36] I. M. Steele, J. V. Smith, and C. M. Skirius, Lunar Planet. Sci. **16,** 817 (1985).
[37] I. M. Steele, Geochim. Cosmochim. Acta **50,** 1379 (1986).
[38] I. M. Steele, J. V. Smith, and C. M. Skirius, Nature London **313,** 294 (1985).
[39] J. L. Berkley, H. G. I. V. Brown, K. Keil, N. L. Carter, J. C. C. Mercier, and G. Huss, Geochim. Cosmochim. Acta **40,** 1429 (1976).
[40] J. L. Berkley, G. J. Taylor, K. Keil, G. E. Harlow, and M. Prinz, Geochim. Cosmochim. Acta **44,** 1579 (1980).
[41] H. Takeda, Earth Planet. Sci. Lett. **81,** 358 (1987).
[42] G. P. Vdovykin, Space Science Rev. **10,** 483 (1970).
[43] J. Akella, R. J. Williams, and O. Mullins, Proc. Lunar Sci. Conf. 7th, 1179 (1976).
[44] E. B. Watson, Amer. Mineral. **64,** 824 (1979).
[45] A. Hashimoto and J. A. Wood, Meteoritics **21,** 391 (1986).
[46] J. A. Wood and A. Hashimoto, Lunar Planet. Sci. **19,** 1292 (1988).
[47] M. Blander and M. Abdel-Gawad, Geochim. Cosmochim. Acta **37,** 701 (1969).
[48] G. Kurat, Lunar Planet. Sci. **17,** 521 (1987).
[49] G. Kurat, Phil. Trans. Roy. Soc. London **A 325,** 459 (1988).
[50] S. Weinbruch, H. Palme, W. F. Mueller, and A. El Goresy, Lunar Planet. Sci. **19,** 1255 (1988).
[51] J. B. Brady and R. H. McCallister, Amer. Mineral. **68,** 95 (1983).
[52] J. Hermeling and H. Schmalzried, Phys. Chem. Minerals **11,** 161 (1984).
[53] G. Arrhenius and B. R. De, Meteoritics **8,** 297 (1973).
[54] G. Kurat, Proc. 27th Internat. Geol. Congr. **11,** 155 (1984).
[55] M. Nazarov, F. Brandstätter, A. A. Ulyanov, G. M. Kolesov, and G. Kurat, Lunar Planet. Sci. **18,** 702 (1987).
[56] J. D. Blum, G. J. Wasserburg, I. D. Hutcheon, J. R. Beckett, and E. M. Stolper, Nature London **331,** 405 (1988).
[57] J. R. Craig, Amer. J. Sci. **273 A,** 496 (1973).
[58] B. R. Frost, J. Petrol. **26,** 31 (1985).
[59] Y. Miura, D. G. W. Smith, and S. Launspach, 8th Symp. Antarct. Meteor., Nat. Inst. Polar Res., Tokyo 1983, p. 8.